LA-UR-97-3670

Title:

ARPES in Strongly Correlated 4f and 5f Systems: Comparison to the Periodic Anderson Model

CONF-970907--

Author(s):

A.J. Arko
J.J. Joyce
L.E. Cox
L. Morales
J. Sarrao
J.L. Smith
Z. Fisk
A. Menovsky
A. Tahvildar-Zadeh
M. Jarrell

MASTER

DISTRIBUTION OF THIS DOCUMENT IS UNLIMITED

Submitted to:

Actinides '97
Baden-Baden, Germany
Sept. 22-26, 2997

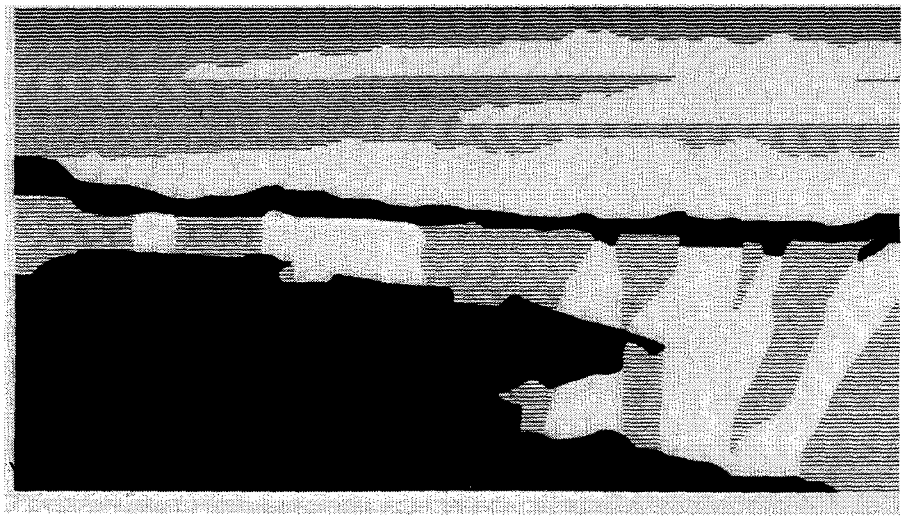

Los Alamos
NATIONAL LABORATOR

DISCLAIMER

ARPES in Strongly Correlated 4f and 5f Systems: Comparison to the Periodic Anderson Model[†,††]

A.J. Arko[a], J.J. Joyce[a], L. E. Cox[a], L. Morales[a], J. Sarrao[a], J.L. Smith[a], Z. Fisk[b], A. Menovsky[c], A. Tahvildar-Zadeh[d], and M. Jarrell[d]

[a]*Los Alamos National Lab., Los Alamos , NM 87545.*

[b]*NHMFL, Florida State Univ., Tallahassee, FL. 32306*

[c]*Natuurkundig Laboratorium, University of Amsterdam, Valckenierstraat 65, 1018 XE Amsterdam, The Netherlands.*

[d]*University of Cincinnati, Cincinnati, Ohio 45221-0011*

Abstract

The electronic structure of both Ce and U heavy fermions appears to consist of extremely narrow, nearly temperature independent bands (i.e., no spectral weight loss or transfer with temperature). A small dispersion of the f-bands above the Kondo temperature is easily measurable so that a Kondo resonance, as defined by NCA, is not evident. Preliminary results, however, indicate that the Periodic Anderson Model captures some of the essential physics. Angle-integrated resonant photoemission results on δ-Pu indicate a narrow 5f feature at E_F, similar in width to f-states in Ce and U compounds, but differing in that cross-section behavior of the near-E_F feature suggests substantial 6d admixtutre.

While U and Ce heavy fermion compounds display nearly identical bulk properties[1], photoelectron spectroscopy (PES) on poly-crystalline specimens indicated possible fundamental differences since the 5f-density of states (DOS), as measured[2] from resonant PES, appeared to be much broader than the corresponding 4f DOS - indeed, much broader even than predicted by band calculations[3]. Further, while a typical Ce heavy fermion spectrum showed several features identified within a Kondo picture[4] as (i) the "main" or f^0 peak at ≈ -2 eV, (ii) the Kondo resonance, i.e. the KR or $4f_{5/2}$, at E_F, and (iii) the Kondo sideband, or the $4f_{7/2}$, at ≈ -0.28 eV, a typical U spectrum measured at resonance in polycrystals showed[2] only a broad featureless triangular structure pinned at E_F. This led to the unsatisfactory situation whereby the single impurity model[5] (SIM) is used to explain Ce compounds (but fails even there to explain single-crystal PES data[6-12]), while identical behavior in U compounds requires another, as yet undeveloped model. Angle-resolved photoemission (ARPES) data on high quality single crystals, however, now indicate that these differences are perhaps only quantitative rather than qualitative, and that narrow dispersive f-bands are observed in both 4f and 5f materials both above and below the characteristic Kondo temperature, T_K. Moreover, these measurements[6-12] consistently find substantive disagreements with predictions of the Non-Crossing Approximation[13] (NCA) and Gunnarsson-Schonhammer[14] solution of the SIM. Most notably, the temperature dependence is far too small, or non-existent, while the spectral weights and widths of the f-features do not scale with T_K (indeed, they appear totally unrelated) in contrast the SIM predictions[13]. While several theoretical approaches[15-20] hold promise of accounting for this behavior, we focus below on the periodic Anderson Model[15], PAM, which in its preliminary stages appears to capture the essential physics. Quite possibly these different approaches, mostly based on the Anderson Hamiltonian, may eventually converge on the same final result, namely some form of renormalized bands[16,17] displaying minimal temperature dependence. A necessary flattening of these bands at E_F with temperature due to the correlations yields the heavy electron mass and yields a semblance of the feature called the Kondo resonance.

The PAM is believed to most correctly describe the strong correlation of electrons in Kondo lattice systems; i.e., stoichiometric compounds with 4f or 5f electrons in the valence shell. Although in the past the SIM has been used as the paradigm for comparison with experimental observations, it cannot account for the coherent nature of electrons (i.e., periodic Bloch states) now observed both above and below T_K. The PAM accounts for these effects. Unfortunately, the difficult nature of PAM calculations necessitates the use of simple generic models rather than real systems. Indeed, the calculation is done in infinite dimensions. Nevertheless some qualitative comparisons between these numerically exact predictions of PAM and experimental data are possible, and indicate qualitative agreement as we show below.

The PAM Hamiltonian on a D-dimensional hypercubic lattice is,

$$
\begin{aligned}
H = {} & \frac{-t^*}{2\sqrt{D}} \sum_{(i,j)\sigma} (d^\dagger_{i\sigma} d_{j\sigma} + h.c.) \\
& + \sum_{i\sigma} (\varepsilon_d d^\dagger_{i\sigma} d_{i\sigma} + \varepsilon_f f^\dagger_{i\sigma} f_{i\sigma}) + V \sum_{i\sigma} (d^\dagger_{i\sigma} f_{i\sigma} + h.c.) \\
& + \sum_i U(n_{fi\uparrow} - 1/2)(n_{fi\downarrow} - 1/2).
\end{aligned}
$$

$+\sum_i U(n_{fi\uparrow} - 1/2)(n_{fi\downarrow} - 1/2).$

In the above equation, $d(f)^{(\dagger)}_{i\sigma}$ destroys (creates) a $d(f)$-electron with spin σ on site I. The hopping is restricted to the nearest neighbors and scaled as $t = t^*/2\sqrt{D}$ (we choose t* = 1, the width of the Gaussian density of states, as the energy scale.) U is the screened on-site Coulomb repulsion for the localized f-states and V is the hybridization between d-and f-states. This model, then, retains the screening and moment formation of the impurity problem, but is further complicated by the lattice effects and the interaction between the moments.

Metzner and Vollhardt[21] observed that the irreducible self-energy and the vertex functions become purely local as the coordination number of the lattice increases. As a consequence, the solution of this interacting lattice model may be mapped onto the solution of a local correlated impurity coupled to an effective bath which is self-consistently determined[22]. The Quantum Monte Carlo (QMC) algorithm of Hirsch and Fye[23] is employed to solve the remaining impurity problem. The basic outputs of this procedure are the f and d Green's functions of the model in Matsubara frequency. The maximum entropy method (MEM) is then employed to analytically continue these functions to real frequency[24].

Initial results indicate a substantial differences between the PAM and SIM approaches, especially in the much slower temperature dependence of PAM[15]. While both models yield a sharp peaking of the DOS at E_F that can be interpreted as a Kondo resonance, the PAM calculations find that these are narrow bands both above and below T_K, as shown in Fig. 1. Here we present the spectral functions for various k-vectors in the simple cubic zone along the cube diagonal, at two different temperatures ($0.62T_K$ and $10T_K$). A d-band at 0.4 filling is allowed to hybridize with a singly occupied f-state, resulting in the two f-d mixed renormalized bands, with a clear hybridization gap. For this system, $U = 1.5$, hybridization $V = 0.6$, while $T_K = 0.02$, in energy units of ω where bandwidth ≈ 1. There is no f-intensity at E_F for $k = (0,0,0)$, the latter developing only at $k = (1,1,1)\pi/2$. As the temperature increases to $10T_K$ there is no loss or transfer of spectral weight from the quasiparticle peaks to the charge transfer peak (still slightly visible at $\omega \approx -1$) as demanded by the SIM. Instead one finds only a broadening of the quasiparticle peaks[15], very much in accordance with experimental results reported previously[6-12]. The charge transfer peak is found to increase with decreasing hybridization, and hence T_K.

The PAM predictions are significantly more consistent with the experimental data than the SIM predictions. While the above calculations most correctly apply to relatively strongly hybridized, cubic Ce systems (i.e., only one f-electron), they appear to be consistent even with relatively low-T_K materials. Indeed, our first observations[8] of periodic effects above T_K were in cubic $CePt_{2.2}$ (T_K < 20K, measurements done at 120K) where the strongest $4f_{5/2}$ signal was obtained for **k** || (1,1,1), and the weakest for **k** || (1,0,0). These results were followed[9] by measurements in the more strongly hybridized $CeBe_{13}$ ($T_K \approx 400K$) where again the weakest signal was for **k** || (1,0,0) and the strongest for **k** || (1,1,1). However, for experimental reasons actual dispersion was not substantiated in those systems. For this reason we show in Fig. 2 ARPES data for tetragonal $CeSb_2$, a ferromagnet below 10K with an estimated T_K of $\approx$3K, where we observed clear evidence of dispersion[11]. The two sets of data in Fig. 2 were taken on different samples at different times. Although LEED was not used for determination of orientation owing to rapid surface deterioration, it is clear that the two data sets represent two different directions in the zone starting from the surface normal. In one case (Fig. 2a) the dispersion is below the Fermi energy, and the rapid decrease of signal strength is now understood as due to a loss of f-admixture in the band below E_F. In the other case (Fig. 2b) the dispersion is above E_F, and one can see that the intensity remains strong despite a large shift of the $4f_{5/2}$ toward E_F. From fig. 1 it is clear that the quasiparticle peak retains, ideed gains, primarily f-character as it disperses above E_F, hence the strong $4f_{5/2}$ peak intensity in Fig. 2b. This data set, then, is understood within the PAM if we allow the possibility that the T_K as determined from SIM parameters ($\approx$ 3 K) is in fact much larger in PAM. Else, there remains a problem.

Similar narrow 5f-bands are also found in uranium systems as seen in the data from a cleaved crystal of antiferromagnetic, tetragonal, USb_2 ($T_N \approx$ 200K) in Fig. 3. The measurements were taken at 20K, hν = 35 eV, and 40 meV resolution. The f-character of bands A and B is deduced from the hν-dependence[25] of their intensity in the left frame where ARPES data at 13° from the sample normal (i.e., from the c-axis) are shown. Only the f-photocurrent increases in this hν range[25], so that features A and B are unquestionably f-related. Note the strong dispersion of band B with hν in the left frame ($\approx$ 600 meV across the zone) which is actually quite different from Ce compounds in its strong dispersion. The similarity to Ce occurs in the near-E_F band A whose 20 to 30 meV of dispersion are more readily seen in the right frame of Fig. 3. Although not evident from Fig. 3, the intensity of the band A quasiparticle peaks drops off dramatically near the c-axis, just as occurs in cubic Ce compounds at the zone center[9], most likely again due to a loss of f-character as it disperses below E_F. The exact strength of the dispersion is masked somewhat by band B which is degenerate with band A near the c-axis, $\theta = 0°$. All this would suggest that the strong correlations are confined to band A and energies very close to E_F.

A most interesting set of ARPES data[11] are shown in Fig. 4 from a cleaved crystal of UPt_3 with a surface normal parallel to the hexagonal or c-axis. The data were taken at 20K, hν = 40 eV and the analyzer rotated in the a-c plane. Several f-related features are observed, again determined to be so from the cross-section dependence on hν, as well as from data at the 5d absorption edge (resonance). The interesting aspect of the data is the complete dissappearance of features A and B between $\theta = 2°$ and $\theta = 3.5°$ analyzer angle. This is precisely where band calculations predict[26] that two f-bands cross E_F. Indeed, band calculations predict the existence of features A, B, C, and D, although the experimental bands appear to be flatter than the calculated bands (our resolution is insufficient to quantify this). The inset of Fig. 4 compares data at $\theta = 1°$ and 25° to emphasize dispersion, though, based on LDA, it is possible that these are actually two different bands.

Inasmuch as the $T_K \approx 10K$ for UPt_3 , these data are taken at twice the Kondo temperature. It thus appears that we are indeed dealing with f-d hybridized renormalized bands, already above T_K, again in qualitative agreement with Fig. 1.

From the above one is led to the conclusion that the electronic structure of both Ce and U compounds is dominated by the existence of extremely narrow f-bands at the Fermi energy, and this already above the characteristic T_K. Temperature dependence studies to 300K in Ce, Yb, and U compounds[6-12] show that these bands are essentially temperature independent with no spectral weight loss, although there is broadening of the features[10.12] and loss due to truncation by the 300 K Fermi function. However, it must be remembered that for very low-T_K materials, or, equivalently, for very high temperatures, the PAM and SIM results again converge. Thus, in order to understand why the f-bands in $CeSb_2$ and $CePt_{2.2}$ remain strong even above 80 K, one must assume that the T_K's determined from the usual SIM parameters are underestimated.

Very weakly hybridized compounds such as UBe_{13} and UAl_2 remain a puzzle. In both cases most of the f-intensity is concentrated in the moderately narrow intense peak near the Fermi energy (see the normal emission UBe_{13} (100) ARPES spectrum in Fig. 5) with no clear evidence of dispersion, while the temperature dependence is nevertheless minimal and no different from high-T_K compounds (not shown). The broad feature at - 0.5 eV in Fig. 5 is also of f-symmetry, but is clearly surface-related since it rapidly diminishes with surface contamination. While there is much speculation about the possibility of multichannel Kondo phenomena responsible for the non-Fermi-liquidUBe_{13} properties, our data cannot shed much light on this since the relatively broad, dispersionless nature of the 5f peak can also result from disorder.

We have also obtained the first ever spectra at resonance for δ-Pu using our newly-comissioned laser plasma light source, more fully described in Ref. 27. In Fig. 6 (bottom spectrum) we show this data taken at hν = 111 eV and compare it to spectra taken at lower photon energies using a helium resonance lamp. There is recent speculation that δ-Pu is a heavy fermion material[28]. However, while a sharp 5f-related feature is indeed evident at the Fermi energy similar to those in Ce and U heavy fermions, the photoelectron cross section would indicate a substantial

6d admixture for this feature[25]. This is evidenced by the fact that the broad peak at -1.7 eV grows more rapidly with photon energy relative to the near-E_F feature. This behavior appears consistent with recent band calculations[29] which predict that the broad -1.7 eV peak is derived from nearly localized pure 5f states, while the near-E_F peak is indeed strongly f-d hybridized. In its present form, the PAM is unable to contribute to the understanding of δ-Pu.

Preliminary results from the PAM calculations, then, suggest that the previous discrepancies encountered between experimental ARPES data and the SIM are substantially diminished with the inclusion of the lattice. The weak temperature dependence, as well as dispersion far above T_K is theoretically reproduced so that PAM is clearly on the right track. However, we cannot yet, on the basis of the present data, rule out other models which are not yet sufficiently developed to make spectral predictions as detailed as the SIM or PAM. Both the charge polaron model of Liu[19] and the two-electron band model of Sheng and Cooper[20] can predict many of the bulk properties. In both models the main parameter is the bandwidth of the weakly hybridized f-bands situated near E_F in the ground state. A source of disccrimination may be the "main" or f^0 peak which is not obtained in Refs. 19 and 20, but may nevertheless occur as a satellite of the photoemission process. The only model that can almost certainly be ruled out is the SIM.

References

† Work Supported by the US Department of Energy

†† Part of work done at SRC which is supported by NSF under award #DMR-95-31009

* Peresent address, Brookhaven National Lab., Upton NY, 11973.

1. G.R. Stewart, 1984, Rev. Mod. Phys. **56**, 755.
2. J.W. Allen, et al., Phys. Rev. Lett. **54**, 2635 (1985).
3. See, for example, R.C. Albers, et al., Phys. Rev. B **33**, 8116 (1986).
4 See, for example, F. Patthey, et al., Phys. Rev. B **35**, 5903 (1987).
5. See various articles in The Handbook on the Physics and Chemistry of the Rare-Earths, vol. 10, K.A. Gschneidner, Jr., L. Eyring and S. Hufner, editors (North Holland, Amsterdam, 1987).
6. J.J. Joyce, et al., Phys. Rev. Lett. **68** 236 (1992).
7. J.J. Joyce,et al., Phys. Rev. Lett. **72**, 1774 (1994).
8. A.B. Andrews, et al., Phys. Rev. B **51**, Rapid Comm., 3277 (1995).
9. A.B. Andrews, et al , Phys. Rev. B **53**, 3317 (1996).
10. J.J. Joyce, et al., Phys. Rev. B **54**, 17515 (1996).
11. A.J. Arko, et al., Phys. Rev. B **56**, Rapid Com., ? (1997).
12. A.J. Arko, et al., Physica B 230-232, 16 (1997).
13. N. E. Bickers, et al., Phys. Rev. B **36**, 2036 (1987).
14. O. Gunnarson and K. Schonhammer in Handbook on the Physics and Chemistry of Rare Earths, Vol. 10, edited by K.A. Gschneider, Jr. L. Eyring and S. Huffner, (Elsevier Publishers, Amsterdam), pp. 103-163, (1987).
15. A.N. Tahvildar-Zadeh, et al., Phys. Rev. B 55, R3332 (1997); A.N. Tahvildar-Zadeh, et al., in preparation.
16. Gertrud Zwicknagl, Advan. Phys. **41**, 203 (1992).
17. M.M. Steiner, et al., Phys. Rev. Lett **72**, 2923 (1994).
18. S.H. Liu, in Handbook on the Physics and Chemistry of Rare Earths, Vol. 17, Ch. 111 (North Holland, Amsterdam, 1993) pp 87-148.
19. S.H. Liu, Physica B240, ? (1997).
20. Q.G. Sheng, and B.R. Cooper, Phil. Mag. Lett. **72**, 123 (1995).
21. W. Metzner and D. Vollhard, Phys. Rev. Lett. **62**, 324 (1989).
22. Th. Pruschke, et al., Adv. in Phys. **42**, 187 (1995), and A. Georges, et al., Rev. mod. Phys. **68**, 13 (1996).

23. J.E. Hirsch and R.M. Frye, Phys. Rev. Lett. **56**, 2521 (1989).
24. M. Jarrell and J. Gubernaitis, Phys. Reports Vol. **269** #3, 133 (1966).
25. **J.J. Yeh and I. Lindau (FINISH REF)**
26. R.C. Albers, et. al., Phys. Rev. B **33**, 8116 (1986).
27. **LIGHT SOURCE FOROM AVS**
28. **Fournier Reference**
29. **J. Wills and O. Eriksson, band calcs**

Figure Captions

1. PAM-derived spectral functions at the indicated points in the simple cubic Brillouin zone, for two indicated temperatures relative to the Kondo temperature. Dark lines indicate partial f-DOS while gray lines indicatepartial d-DOS. Note that the narrowest features, both f and d, are at the Feri energy.

2. ARPES spectra for $CeSb_2$, with all analyzer angles measured relative to the surface normal, i.e., (001). **(a)** Spectra with k// along the (100) direction are shown for hv = 40 eV. Note the dispersion to energies below E_F. **(b)** Spectra taken along a different direction, possibly along (110), show dispersion toward higher energies. Note that the 4f-spectral weight remains strong.

3. ARPES spectra for USb_2, with all analyzer angles measured relative to the surface normal, i.e., (001). **(a)** Spectra at indicated photon energies, but at constant 13° from normal. Note the rapid growth of intensity for features A and B, indicatinf f-character. (b) Spectra at h_n = 35 eV but at varying analyzer angles, to show dispersion of band A.

4. ARPES spectra at hv = 40 eV and T = 20 K for UPt_3 at the indicated points in the Brillouin zone. The data, taken at twice $_{TK}$, show huge variation with momentum. Note the sudden dissappearance of peak A at 3.5°, precisely where LDA predicts dispersion above E_F. Inset emphasizes the dramatic difference in both peak position and intensity between 1° and 25°.

5. Normal emission spectrum of UBe13 at hn = 48 eV. The feature at -0.5 eV was observed to dissappear with 1 Langmuir of oxygen doping, and is thus presumed due to the surface. Only the 6d states display actual dispersion.

6. Angle-integrated spectra of d-Pu at the indicated photon energies. The near-resonance spectrum at hv = 111 eV was taken with light from a laser plasma light source. The spectral weight of the near-E_F peak increases slower with hv than the feature at -1.7 eV and is thus assumed to contain 6d admixture in the DOS. The -1.7 eV feature is believed due to nearly localized 5f states.

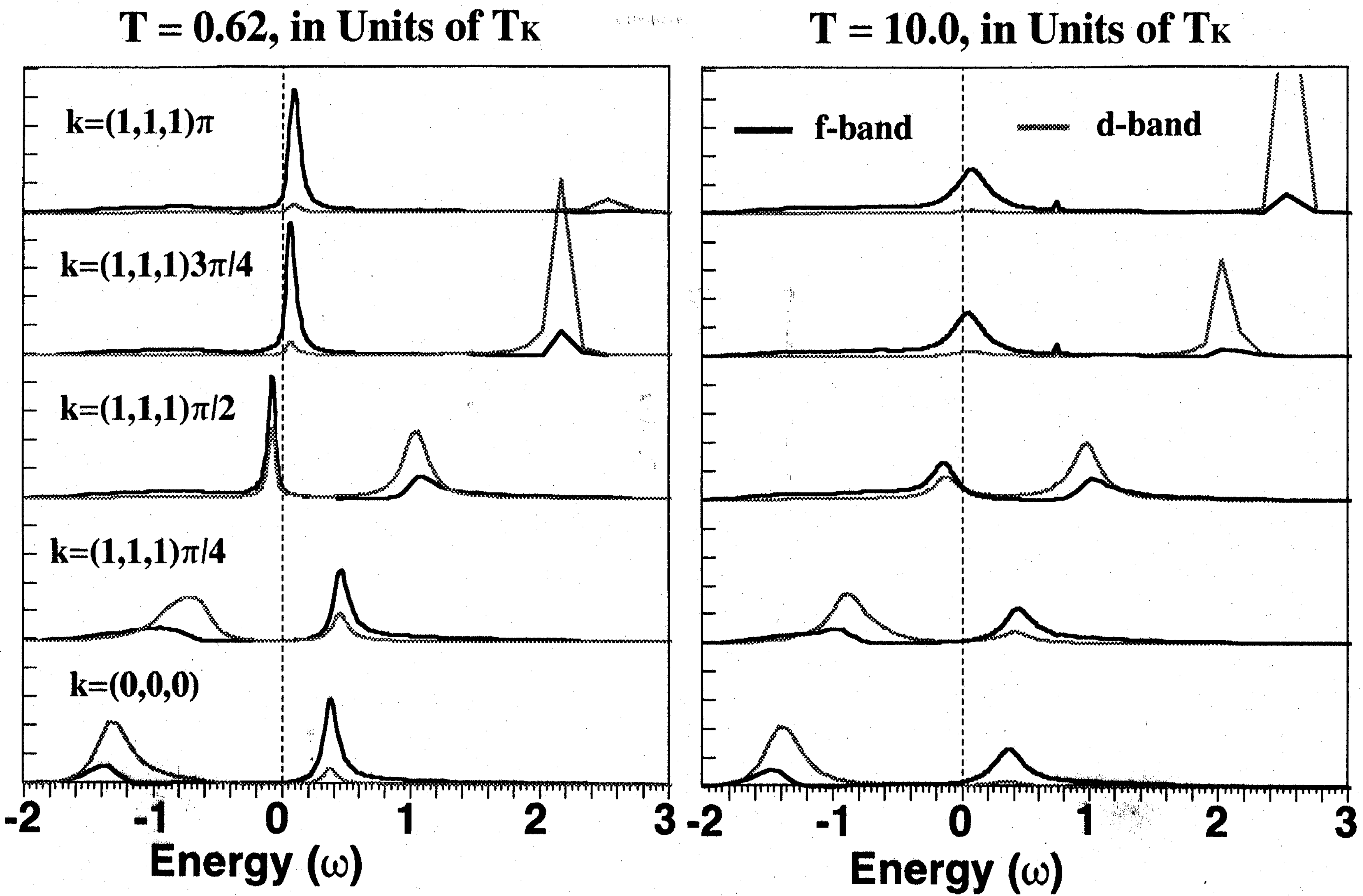
T = 0.62, in Units of Tк
T = 10.0, in Units of Tк
f-band
d-band
k=(1,1,1)π
k=(1,1,1)3π/4
k=(1,1,1)π/2
k=(1,1,1)π/4
k=(0,0,0)
-2
-1
0
1
2
3
Energy (ω)

Fig. 1

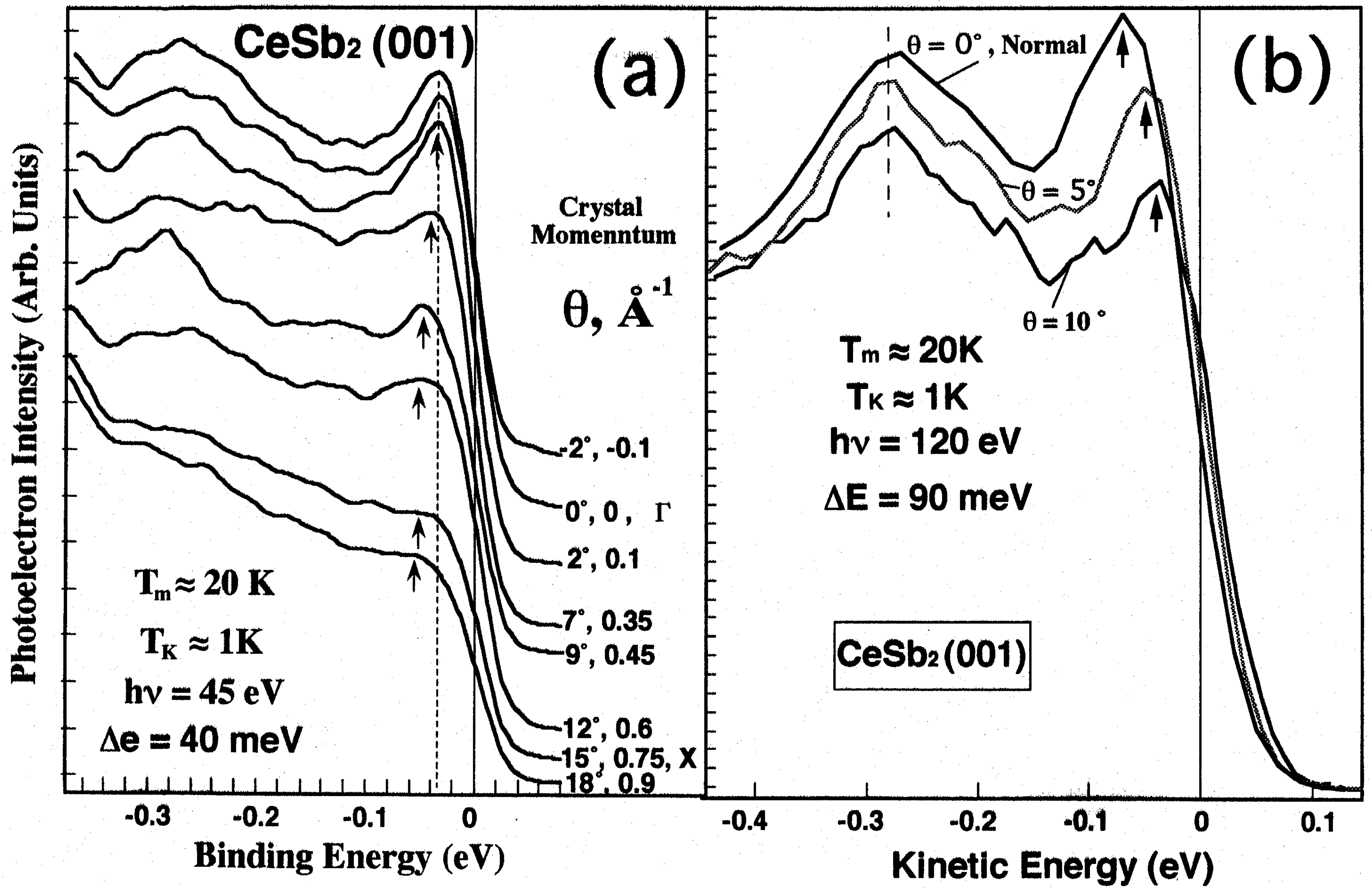
CeSb₂ (001)
(a)
Crystal Momenntum
θ, Å⁻¹
-2°, -0.1
0°, 0 , Γ
2°, 0.1
7°, 0.35
9°, 0.45
12°, 0.6
15°, 0.75, X
18°, 0.9
Tm ≈ 20 K
TK ≈ 1K
hν = 45 eV
Δe = 40 meV
-0.3
-0.2
-0.1
0
Binding Energy (eV)
Photoelectron Intensity (Arb. Units)
(b)
θ = 0°, Normal
θ = 5°
θ = 10 °
Tm ≈ 20K
TK ≈ 1K
hν = 120 eV
ΔE = 90 meV
CeSb₂ (001)
-0.4
-0.3
-0.2
-0.1
0
0.1
Kinetic Energy (eV)

Fig. 2

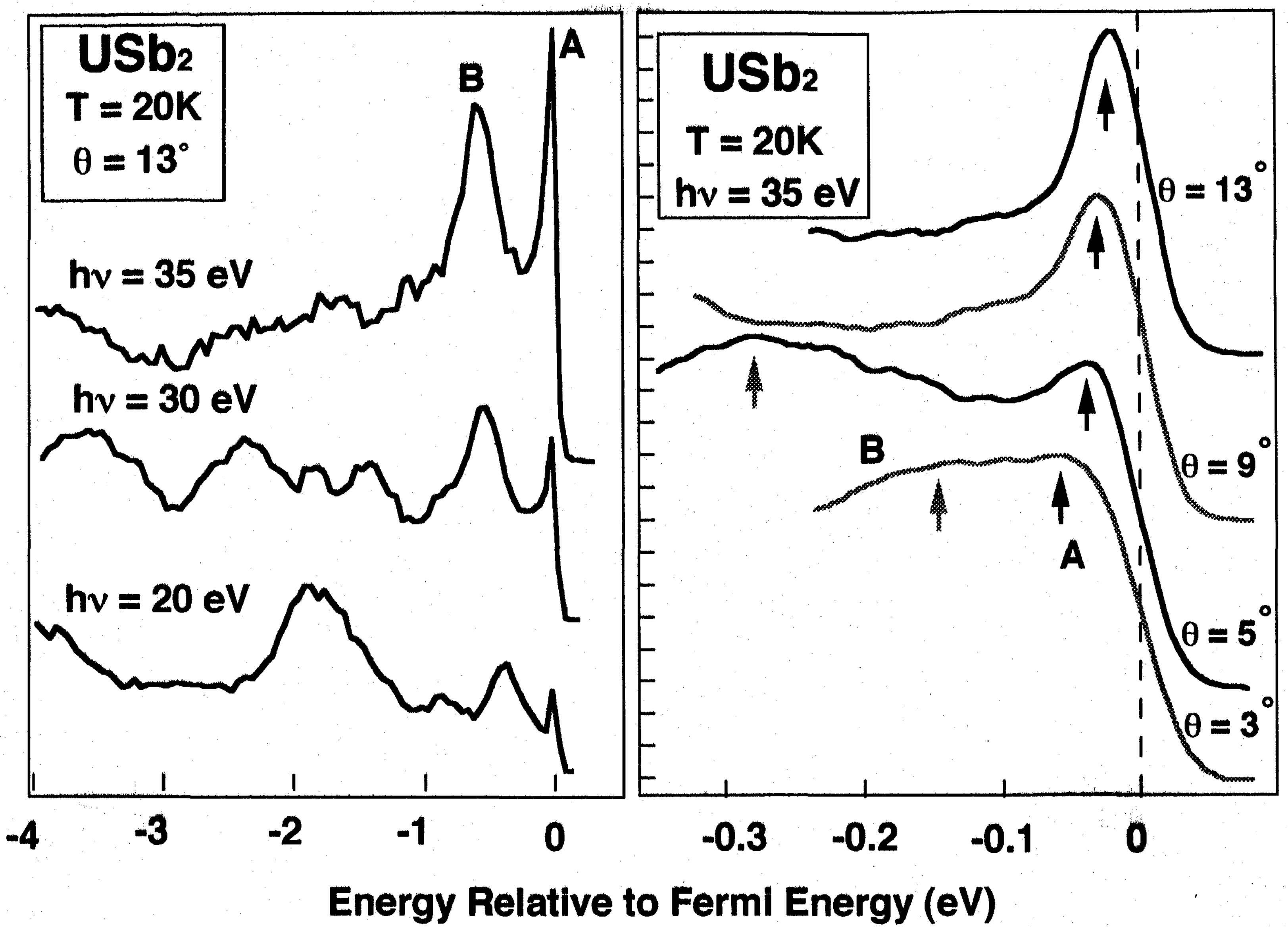
USb2
T = 20K
θ = 13°
B
A
hν = 35 eV
hν = 30 eV
hν = 20 eV
-4
-3
-2
-1
0
USb2
T = 20K
hν = 35 eV
θ = 13°
θ = 9°
θ = 5°
θ = 3°
B
A
-0.3
-0.2
-0.1
0
Energy Relative to Fermi Energy (eV)

Fig. 3

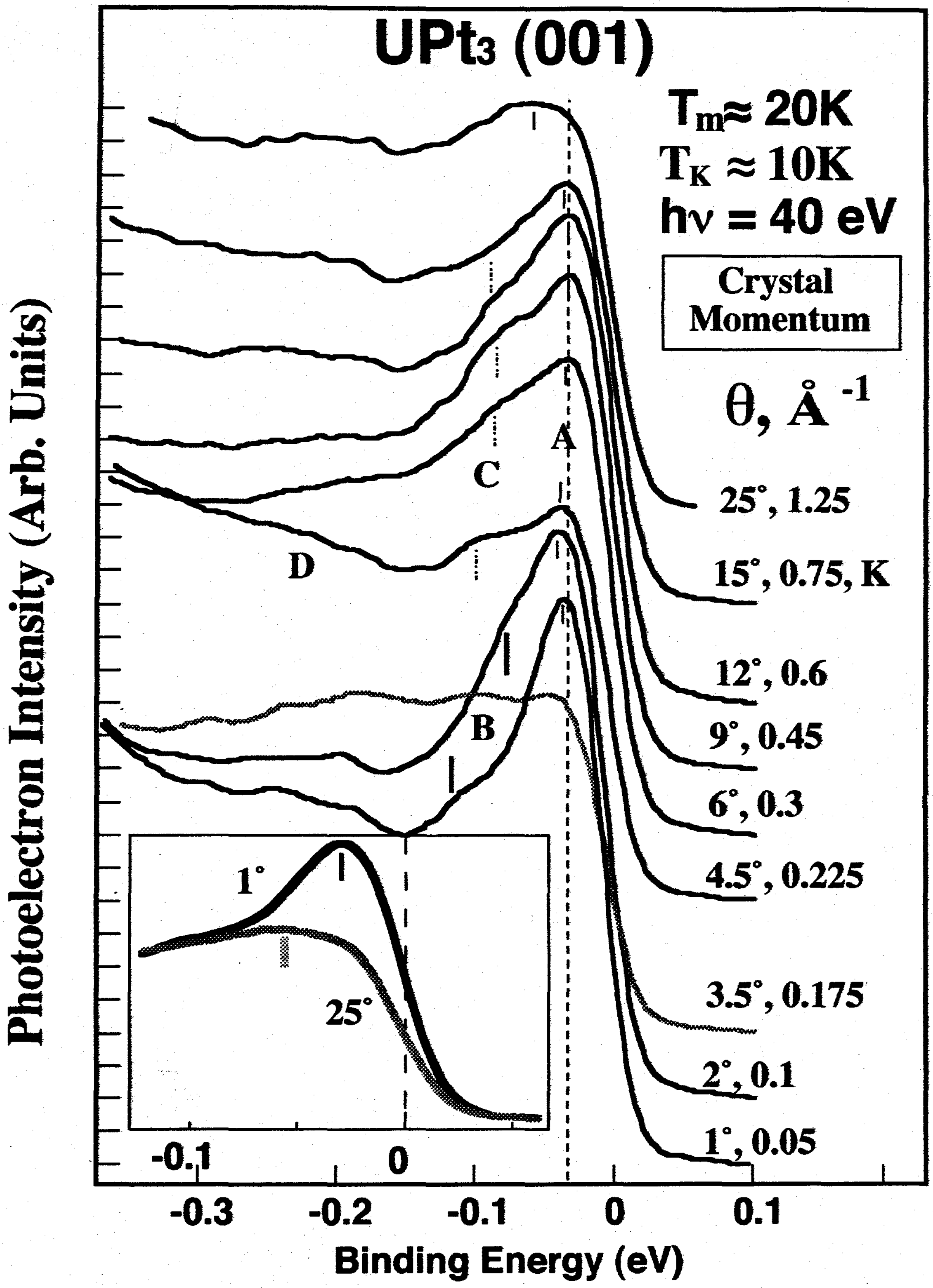
UPt3 (001)
Tm≈ 20K
TK ≈ 10K
hν = 40 eV
Crystal Momentum
θ, Å -1
A
B
C
D
25°, 1.25
15°, 0.75, K
12°, 0.6
9°, 0.45
6°, 0.3
4.5°, 0.225
3.5°, 0.175
2°, 0.1
1°, 0.05
1°
25°
-0.1
0
-0.3
-0.2
-0.1
0
0.1
Photoelectron Intensity (Arb. Units)
Binding Energy (eV)

Fig. 4

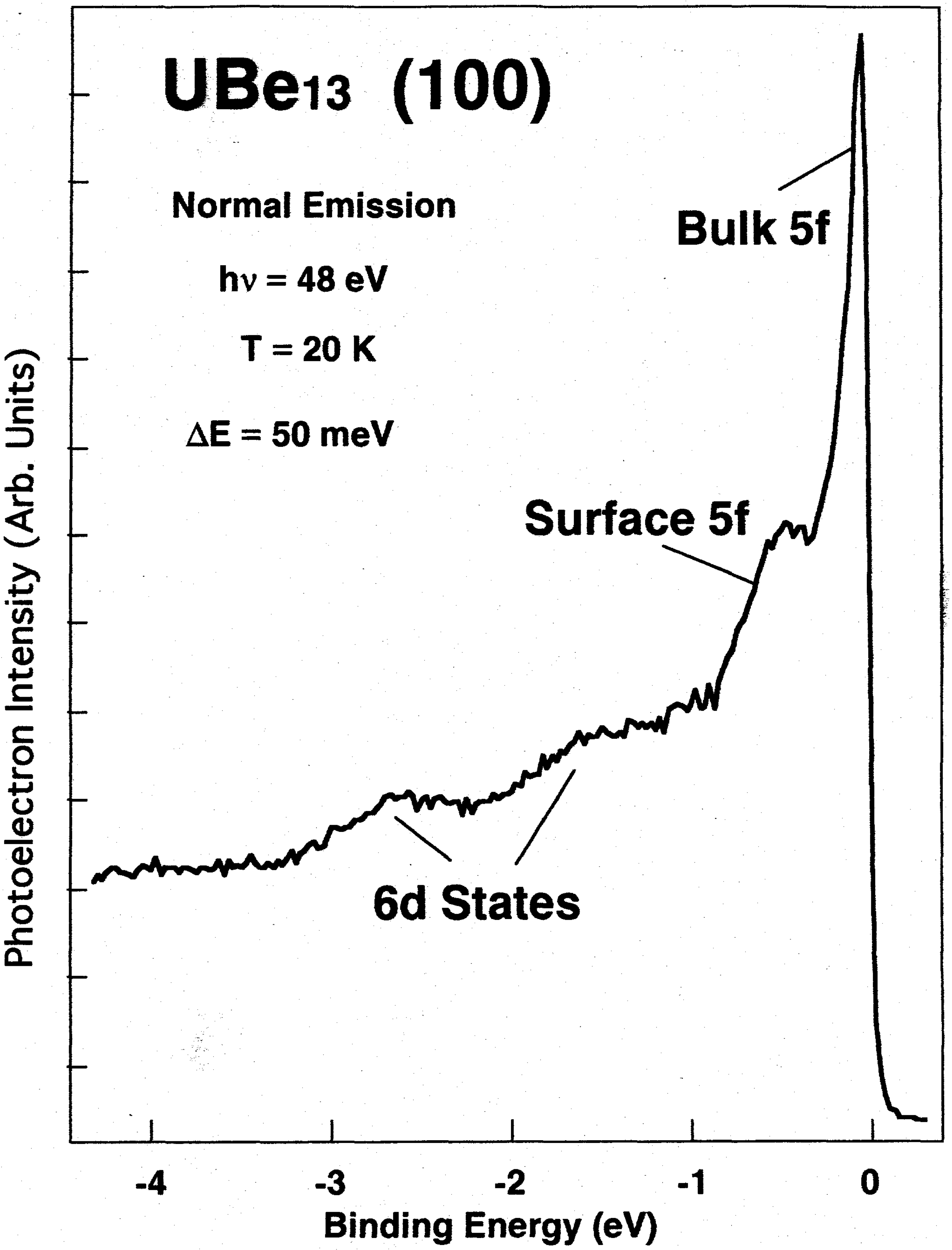
UBe13 (100)
Normal Emission
hν = 48 eV
T = 20 K
ΔE = 50 meV
Bulk 5f
Surface 5f
6d States
Photoelectron Intensity (Arb. Units)
-4
-3
-2
-1
0
Binding Energy (eV)

Fig. 5

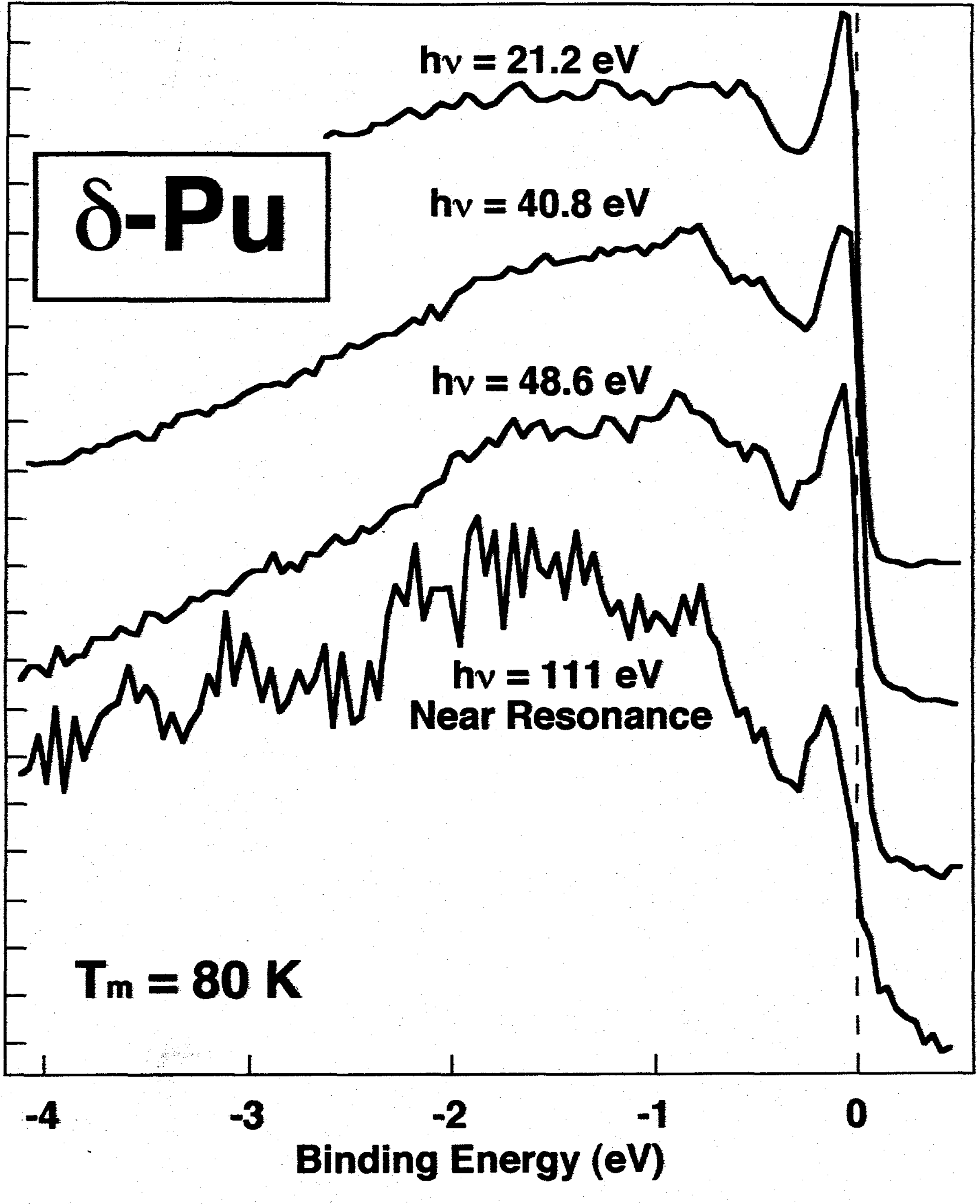
δ-Pu
hν = 21.2 eV
hν = 40.8 eV
hν = 48.6 eV
hν = 111 eV
Near Resonance
Tm = 80 K
-4
-3
-2
-1
0
Binding Energy (eV)